

## Melting of Crystalline Confined Plasmas

J. P. Schiffer

*Physics Division, Argonne National Laboratory, Argonne, Illinois 60439  
and The University of Chicago, Chicago, Illinois 60637*

(Received 23 January 2002; published 6 May 2002)

The melting of cold, ordered arrays of up to 10 000 charges, confined in external fields, has been studied in simulations. The latent heat associated with melting and the behavior of the specific heat were obtained, along with the spatial correlation function  $g(r)$  with respect to neighbors and the diffusion rates, both as a function of temperature. The melting temperatures of finite arrays of ions are found to be lower than that for infinite Coulombic matter, by an amount that depends on the number of charges and on the fraction of ions in the surface layer, in particular.

DOI: 10.1103/PhysRevLett.88.205003

PACS numbers: 52.27.Gr, 36.40.Ei, 52.27.Jt

The fact that an infinite array of like charges forms an ordered state has been known for a long time [1] and has been explored in computer simulations since the early days of large-capacity computers [2,3]. The form of ordering is body centered cubic for infinite Coulombic matter. Simulations have shown [2–5] that there is a phase transition from order to a liquid state at a well-defined temperature of  $T \cong 1/173$  in units of  $q^2/a_{\text{WS}}$  (where  $q$  is the charge and  $a_{\text{WS}}$  is the Wigner-Seitz radius, with  $4/3\pi a_{\text{WS}}^3 = 1/\rho$ ,  $\rho$  being the density). Since the properties of these Coulomb systems scale with density, it is customary to define the reciprocal temperature in terms of the dimensionless quantity  $\Gamma$ :

$$\Gamma \equiv \frac{q^2/a_{\text{WS}}}{kT}, \quad (1)$$

where  $k$  is Boltzmann's constant. The latent heat associated with this phase transition has also been explored (see, for instance [5]). Note that  $\Gamma$  is a dimensionless parameter where the temperature depends on the density. At the densities typical of ion traps where  $a_{\text{WS}} \approx 10\mu$  this transition takes place in the milliKelvin regime. For a general review of the properties of such plasmas, see [6].

Finite clouds of ions show ordered structures with a different form of ordering. For instance, with a harmonic (and isotropic) confining potential that is representative of ion traps, cold particles form a cloud with a well-defined surface, constant macroscopic density, with well-defined concentric shells in the interior [7]. The surface layer and each (equally spaced) shell contain ions in a pattern of equilateral triangles. The triangles in the different shells cannot align perfectly; the pattern is reminiscent of the "hexatic" ordering in liquid crystals. Such ordering in trapped ions has been observed in simulations [7,8] and in the laboratory [9]. For spherical clouds containing more than about 20 000 ions, there are some 20 or so concentric shells, but then, for larger clouds, bcc ordering that is characteristic of infinite matter appears again in the interior [10].

The melting of such finite clouds had not been studied previously. While a finite system cannot form a sharp phase transition, there clearly is a transition between a dis-

ordered and an ordered phase. Figure 1 displays the pattern of the outer two shells for an isotropically confined 10 000-ion system, its radial density, and the spatial correlation function  $g(r)$  from molecular dynamics simulations at three temperatures: frozen, liquid, and gaseous. The transition from order to disorder might be expected to be different from that in infinite matter, both because the system is finite and because the form of ordering is different. This is the first report of such studies and may serve as a guide to future experiments and as a prototype for melting of finite systems with a long-range interaction.

Simulations have been carried out for a system of 10 000 ions that was allowed to find a minimum in its potential energy by allowing the particles to propagate forward in time, gradually converting potential energy into kinetic energy, and then scaling down velocities. This procedure was repeated until the system reached a value of  $\Gamma$  of about 30 000.

Starting with such a cold system, predetermined increments of energy were added. In each successive step the previous (colder) spatial configuration was used, and each ion was assigned a random velocity picked from a Maxwell-Boltzmann distribution with the desired new mean energy. The system was then allowed to propagate for a sufficiently long time to establish a new equilibrium as the increase in kinetic energy dissipated partially into potential energy. The simulation had to be run for a sufficiently long time to ensure that the new equilibrium values could be extracted with reasonable accuracy. At the lowest temperatures, up to 1000 plasma periods or  $\sim 100\,000$  time steps were required to establish an equilibrium value with confidence, while above the melting temperature equilibration was faster. Energy increments were smaller in the vicinity of the melting point and larger elsewhere.

The potential energy  $U$  is

$$U \equiv \sum_i 1/2Kqr_i^2 + \sum_{\substack{i,j \\ i \neq j}} q^2/r_{ij} - U_0, \quad (2)$$

where  $Kq$  is the harmonic force constant of the (isotropic) confinement,  $r_i$  are the radial coordinates of the ions with respect to the origin,  $r_{ij}$  are the separations between pairs

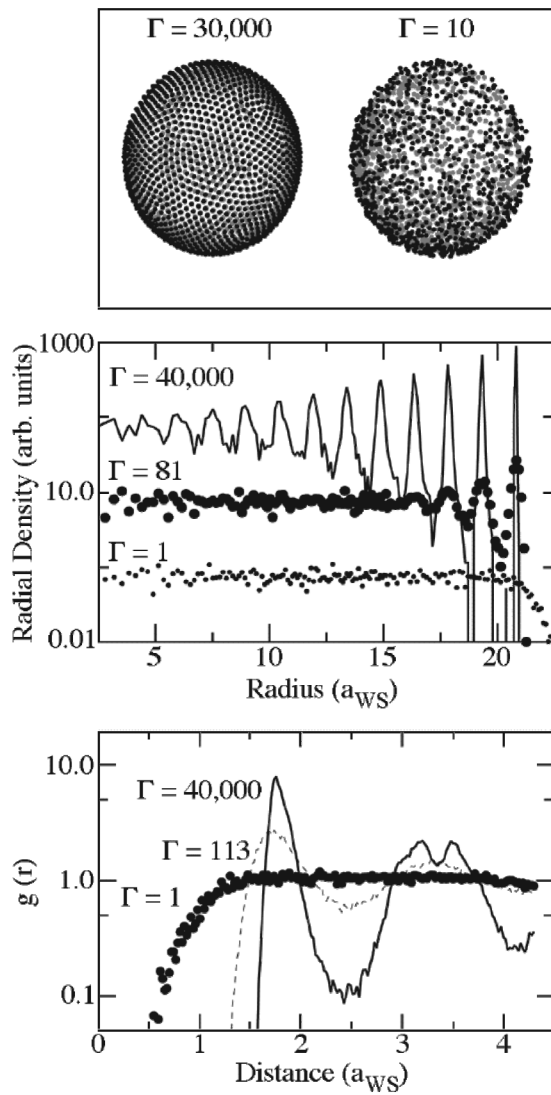


FIG. 1. On top, the outer two layers of ions are displayed for a 10 000-ion system. The ions in the outermost layer are shown in black, and the next layer in gray. On the left, a cold, ordered array is shown, while on the right a disordered one at high temperature, with the ions in corresponding radial intervals shown. The middle box shows the radial density within the ion cloud at three different temperatures with the vertical scales displaced for visibility. On the bottom, the correlation function  $g(r)$  is shown, at the three temperatures. For the lower two boxes the distance scale is in units of the Wigner-Seitz radius  $a_{WS}$ .

of particles, and  $U_0$  is the minimum of potential energy found by extrapolating the results to zero temperature. This zero may not be the “true” ground state of this system [11]; however, the energy differences between minima in the potential-energy surface are negligibly small in the present context. The behavior of the potential energy (divided by the temperature), as a function of kinetic energy is shown in Fig. 2 together with the specific heat  $C = \Delta H/\Delta T$ , where  $H$  is the total heat content of the system (in the ideal gas limit,  $C = 3/2$ , while at low temperatures, where potential and kinetic energies are equal,  $C = 3$ ).

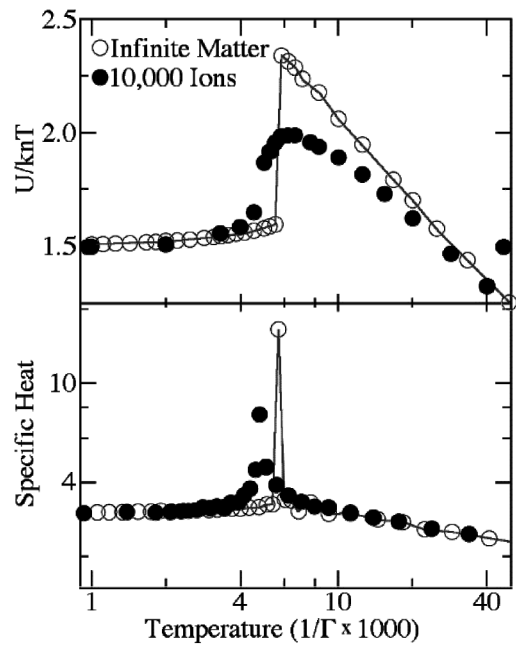


FIG. 2. The total energy of a system of charges is shown on top for an infinite system of ions from Ref. [5] as open circles, and for a 10 000-ion system as filled circles. The lower plot is the corresponding specific heat. Note that at low temperatures both approach the value of 3.0. The temperature scale is in units of  $1/\Gamma$ .

It is evident from Fig. 2, showing the potential energies and specific heat, that there is a melting temperature in the 10 000 ion system similar to that in infinite Coulombic matter, though it is somewhat smeared out and shifted to a lower temperature. Three other measures of this transition are shown in Fig. 3: the ratio of the maximum to the minimum in the correlation function  $g(r)$ , the ratio of the density in the outer six shells to the density in the valleys between shells, and the diffusion coefficient

$$D = \sum_i d_i^2 / (2N \Delta t), \quad (3)$$

where  $d_i$  is the three-dimensional displacement of each ion in the time interval  $\Delta t$  and  $N$  is the number of ions. All of these show an anomaly at the transition temperature.

The behavior of diffusion is shown in more detail in Fig. 4, where in the top plot it is evident that diffusion follows a pattern—presumably particles move easier in areas where the imperfect lattice on the spherical surface has defects. In the center panel the relative constancy of the overall diffusion coefficients with radius is shown. Finally, on the bottom, the ratio of the tangential component of diffusion *within* shells to the radial one *between* shells is plotted, showing an anomaly near the melting temperature in the outer region that is not present in the interior. This is in qualitative agreement with the observation of [8], where in a simulation of magnetic confinement of a smaller (256-ion) system, no radial diffusion was seen.

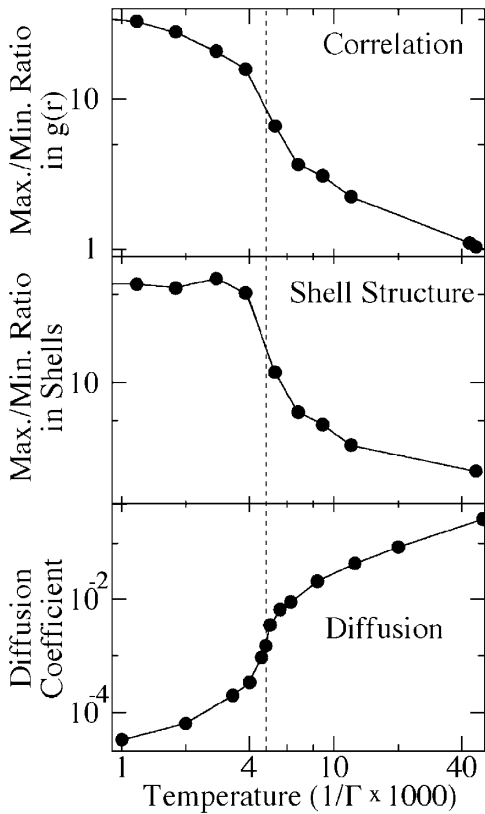


FIG. 3. Three properties of the ion clouds are shown that depend on temperature. The top figure is the ratio of densities in the shells to those in the gaps between shells, as a function of temperature for the outer five shells. In the middle, the ratio of the first peak to the following minimum in  $g(r)$  (the two-dimensional correlation function of the type that was shown in Fig. 1) is plotted as a function of temperature. Finally, the bottom plot is that of the (three-dimensional) diffusion coefficient in the ion clouds as a function of temperature. The dashed line, in each box, corresponds to the temperature where the specific heat shows a maximum for 10 000 ions.

The simulations reported so far were for plasmas confined by a constant force. In rf quadrupole confinement (Paul traps and accelerator storage rings) particles are confined in an alternating rf focusing field whose frequency is fast compared to the plasma frequency. The effective temperature in such systems, defined as the motion of particles in complete rf cycles, and the coupling of energy from the rf motion into random temperaturelike motion can be very small at low temperatures [12]. A simulation was tried for 1000 ions confined in an rf field, as in [12], and the specific heat peaked at the same value as that for a steadily confined one.

Finally, the question was addressed whether the lowering of the melting temperature was the consequence of the different form of ordering, or of the finite size. Figure 5 shows results that include calculations for 10 000-, 1000-, and 100-ion systems, as well as for Coulombic matter. The anomaly in specific heat is progressively weaker with a decreasing number of ions, but the peak is clearly shifting to

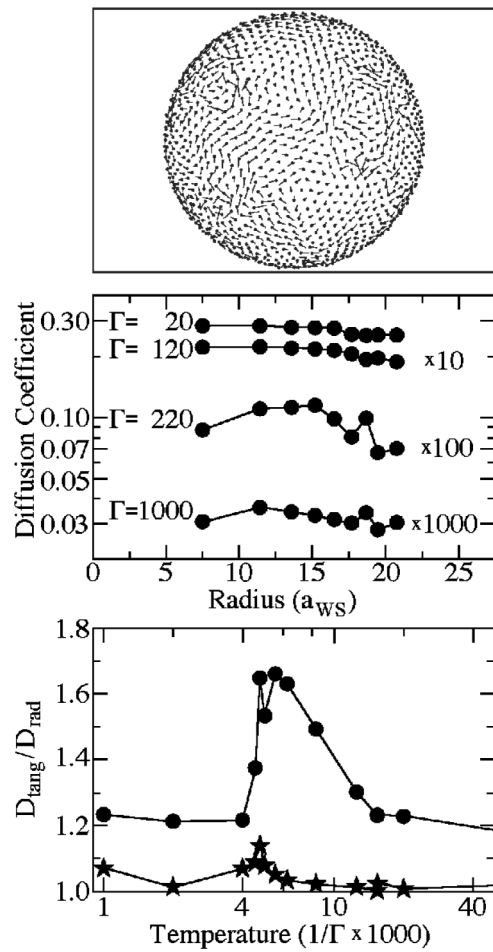


FIG. 4. The upper figure displays the outer shell of ions as dots, at a temperature near melting ( $\Gamma = 220$ ), with the lines representing the distance each ion traveled in the time interval of  $[1/\omega_{pi}]$ . The middle box displays the (three-dimensional) diffusion coefficient  $D$  in units of  $[a_{ws}^2 \times \omega_{plasma}]$  as a function of radius. The lowest box shows the ratio of the (one-dimensional) component of the diffusion coefficient along the spherical shells to the radial component perpendicular to it, with the solid dots representing the outer 50% of the array, and the stars the inner part.

lower temperatures. The fact that the data show a smooth size dependence indicates that this lowering is probably a size effect—the energy differences between bcc and shell structures [11] are 3–4 orders of magnitude smaller than the latent heat. Since the ions on the outer surface have no neighbors on one side, the lowering of the melting temperature is plotted against the fraction of ions residing on the outermost surface. The lowering of temperature appears to be linear with this fraction—starting from the infinite medium. (Note that for 60 ions, 48 are in the outer shell; for 12 ions, all ions are on the outside, as was found in [13].) Thus, it would appear that the lowered melting temperature is almost entirely due to the finite size rather than the different form of ordering. Such a dependence in the melting temperature has not yet been observed in measurements but will perhaps be possible with present

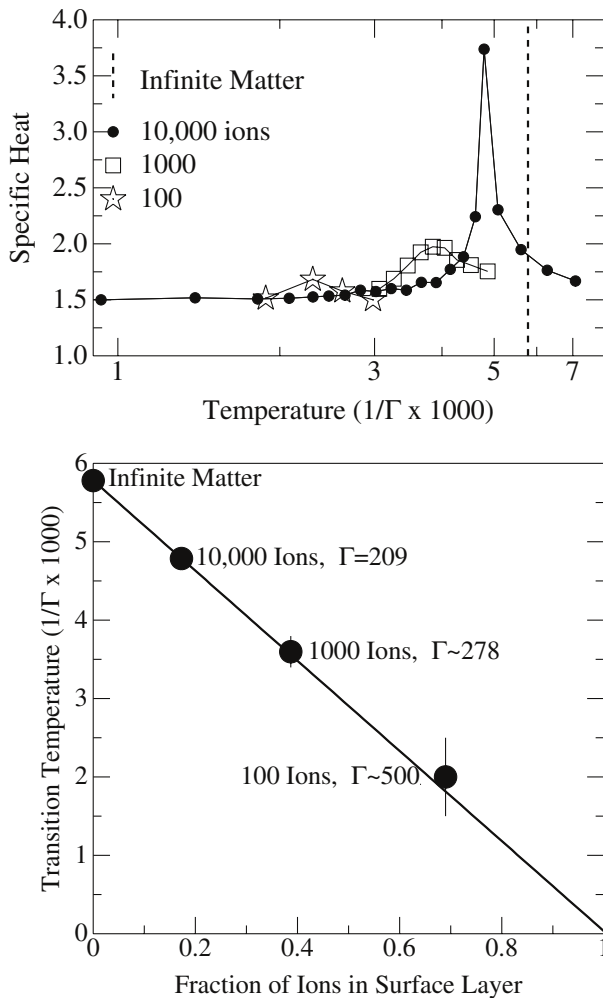


FIG. 5. Specific heat plots of the type that was shown in Fig. 2 for 10000, 1000, and 100 ions. The peak is weaker for the smaller clouds and shifted to lower temperatures. The lower plot shows the temperature at which the specific heat has its maximum value, plotted against the fraction of ions in the cloud that is in the outermost shell; the error bars indicate the uncertainty with which the position of the peaks can be deduced. This dependence seems to obey the linear relationship  $T_{\text{melting}} = 1/\Gamma_0 \times (1 - 0.98 \times F)$  (where  $\Gamma_0$  is the melting point of infinite Coulombic matter, and  $F$  is the fraction of ions in the outer layer) shown as the line.

techniques. A lowering of the melting temperature in finite atomic clusters (where the interaction is short range

and the functional dependence does not appear to be so simple) has been known for some time [14]. The present system, with the ordering arising only from Coulomb interactions, may give rise to the particularly simple behavior found here.

In conclusion, the melting of confined, finite plasmas is different from that of infinite Coulombic matter, apparently due to the inevitable fact that these clusters have a surface. The decrease in melting temperature appears to be proportional to the relative size of the surface layer and becomes less sharply defined for smaller systems. The diffusion rates in the outer regions are substantially larger parallel to the surface than perpendicular to it, in the vicinity of the melting temperature.

This research was supported by the U.S. Department of Energy, Nuclear Physics Division, under Contract No. W-31-109-ENG-38.

- 
- [1] E. Madelung, Phys. Z. **19**, 524 (1918).
  - [2] S. G. Brush, H. L. Sahlin, and E. Teller, J. Chem. Phys. **45**, 2102 (1966).
  - [3] E. L. Pollock and J. P. Hansen, Phys. Rev. A **8**, 3110 (1973).
  - [4] W. L. Slattery, G. D. Doolen, and E. H. DeWitt, Phys. Rev. A **26**, 2255 (1982).
  - [5] R. T. Farouki and S. Hamaguchi, Phys. Rev. E **47**, 4330 (1993).
  - [6] D. H. E. Dubin and T. M. O'Neil, Rev. Mod. Phys. **71**, 87 (1999).
  - [7] A. Rahman and J. P. Schiffer, Phys. Rev. Lett. **57**, 1133 (1986).
  - [8] D. H. E. Dubin and T. M. O'Neil, Phys. Rev. Lett. **60**, 511 (1988).
  - [9] S. L. Gilbert, J. J. Bollinger, and D. J. Wineland, Phys. Rev. Lett. **60**, 2022 (1988).
  - [10] X.-P. Huang, J. J. Bollinger, T. B. Mitchell, and W. M. Itano, Phys. Rev. Lett. **80**, 73 (1998).
  - [11] H. Totsuji, T. Kishimoto, C. Totsuji, and K. Tsuruta, Phys. Rev. Lett. **88**, 125002 (2002).
  - [12] J. P. Schiffer, M. Drewsen, J. S. Hangst, and L. Hornekaer, Proc. Natl. Acad. Sci. U.S.A. **97**, 10697 (2000).
  - [13] R. Rafac, J. P. Schiffer, J. S. Hangst, D. H. E. Dubin, and D. J. Wales, Proc. Natl. Acad. Sci. U.S.A. **88**, 483 (1991).
  - [14] P. Buffat and J. P. Borel, Phys. Rev. A **13**, 2287 (1976).